Size Effects on Magnetic Property and Crystal Structure of Mn3O4 Nanoparticles in Mesoporous Silica

doi: http://dx.doi.org/10.1109/TMAG.2018.2859950

SIZE EFFECTS ON MAGNETIC PROPERTY AND CRYSTAL STRUCTURE OF Mn_3O_4 NANOPARTICLES IN MESOPOROUS SILICA

Takayuki Tajiri[1], Koji Sakai[2], Hiroyuki Deguchi[2], Masaki Mito[2], and Atsushi Kohno[1]

[1] Faculty of Science, Fukuoka University, Fukuoka 814-0180, Japan
[2] Graduate School of Engineering, Kyushu Institute of Technology, Kitakyushu 804-8550, Japan

Mn_3O_4 nanoparticles with particle sizes of 7.8, 11.4, and 18.3 nm were synthesized in the pores of mesoporous silica, and their crystal structure and magnetic properties were investigated. The powder X-ray diffractions at room temperature indicated that the crystal structural symmetry was the same as that for bulk crystal, and the lattice constants deviated from those for bulk crystal, which depended on the particle size. In addition, compared with the bulk crystal, the Jahn-Teller distortion for the nanoparticles was suppressed and decreased with decreasing the particle size. The coercive field for 7.8 nm was rather smaller than those for 11.4 and 18.3 nm. The nanoparticles with 11.4 and 18.3 nm exhibited pronounced three kinds of magnetic transition temperatures, whereas the susceptibility for 7.8 nm indicated the existence of two transition temperatures. These experimental results suggested that the Mn_3O_4 nanoparticles have a strong correlation between crystallographic structure and magnetic property, and the characteristic magnetic size effects are attributed to the reduction of Jahn-Teller distortion.

Crystal structure, Lattice distortion, magnetic property, Nanoparticles

I. INTRODUCTION

Spinel oxides with a general formula AB_2O_4 has tetrahedral A site with four oxygen and octahedral B site with six oxygen arranged in a pyrochlore latteice. When magnetic ions occupy the B site, geometric magnetic frustration often occurs owing to the strong antiferromagnetic interactions between B sites. The Mn_3O_4 has geometrical frustration derived from the antiferromagnetic interactions between the B sites of spinel oxide. Mn_3O_4 exhibits interesting phenomena such as magnetodielectric, magnetoelastic and magnetocaloric behaviors, and successive phase transformations owing to the strong coupling among spin, orbital, and lattice degrees of freedom [1-6]. For Mn_3O_4, the tetrahedral A sites and octahedral B sites are selectively occupied by Mn^{2+} and Mn^{3+} ions, respectively. Since Mn^{3+} ions at the MnO_6 octahedral site with one electron in the doubly degenerate e_g states, Mn_3O_4 exhibits a structural phase transition from cubic to tetragonal at 1443 K due to the strong instability of the Jahn-Teller distortion, whose magnitude is estimated to be $c/\sqrt{2}\ a \sim 1.16$ based on the ratio of lattice constants ($a \sim 5.76$ Å and $c \sim 9.47$ Å) [4,5]. The Mn_3O_4 bulk crystal exhibits a ferrimagnetic ordering, called Yafet-Kittel phase, at $T_N = 42$ K, where the magnetic moments are oriented along the [110] direction. In addition, as temperature decreases, the magnetic phase of Mn_3O_4 changes successively to an incommensurate (IC) phase at $T_1 = 40$ K, and finally to a commensurate phase, called cell-doubled (CD) phase at $T_2 = 34$ K, where the magnetic unit cell is doubled along the [110] direction from that of the original cubic spinel structure.

The nanoparticle of strongly correlated materials such as manganese oxide are expected to exhibit characteristic size effects on crystal structure and magnetic property owing to the strongly electron correlation and strong coupling among spin, orbital, and lattice. In fact, we have already shown that nanoparticles of strongly correlation materials, $LaMnO_3$[7], $DyMnO_3$ [8], and NiO [9], exhibit characteristic size dependences on the magnetic properties and crystallographic structures. These nanoparticles exhibit the remarkable changes in crystallographic structure, i.e., changes in the structural symmetry, lattice constant, and lattice strain, which induces the unique size effects of magnetic properties. Moreover, the nanoparticles of the magnetically frustrated materials are expected to the characteristic size effects. The nanoparticles of $DyMn_2O_5$, which has magnetic frustration owning to the intricate interplay of at least five magnetic Mn-Mn spin interactions in the geometrically frustrated structure, exhibit the unusual magnetic size effect derived from the distortion on the crystallographic structure [10].The magnetic properties for the Mn_3O_4 nanoparticles are expected to be different from those for bulk crystal owing to the modulation of magnetic frustration and lattice distortion due to the surface effect. In this study, we synthesized the Mn_3O_4 nanoparticles with particle size of approximately 8-18 nm in the pores of mesoporous silica, and their crystallographic structure and magnetic properties were investigated. These results suggested the existence of the strong correlation between magnetic properties and lattice distortion associated with Jahn-Teller distortion in the Mn_3O_4 nanoparticles.

II. EXPERIMENT

Mn_3O_4 nanoparticles were synthesized in the pores, with a diameter of approximately 7 nm, of mesoporous silica SBA-15. SBA-15 was used as a template to equalize the particle size in the fabrication of the Mn_3O_4 nanoparticles and to deflocculate synthesized nanoparticles since it has a two-dimensional hexagonal mesoporous structure and its pores are separated by silica wall [11]. The Mn_3O_4 nanoparticles were synthesized by soaking the SBA-15 in a aqueous solution of $MnCl_2{\cdot}4H_2O$. The soaked SBA-15 was then dried and calcinated in an air atmosphere. The powder X-ray diffraction (XRD) measurements for the synthesized nanoparticles were carried out at room temperature by using a synchrotron radiation X-ray diffractometer with a Debye-Scherrer camera at the beamline BL-8B at the Photon Factory (PF) of the Institute of

Materials Structure Science, High Energy Accelerator Research Organization (KEK). The X-ray wavelength was calibrated using the XRD pattern of CeO_2 powder. The magnetic properties of the nanoparticles were investigated by using a superconducting quantum interference device (SQUID) magnetometer (Quantum Design Inc.). Temperature dependence of DC susceptibility and magnetization curves were measured.

III. Experimental results and discussion

We observed powder XRD patterns for the synthesized Mn_3O_4 nanoparticles in the pores of SBA-15 at room temperature, as shown in Fig. 1. The diffraction patterns of three Mn_3O_4 nanoparticles exhibited broad Bragg peaks, which were attributed to the tetragonal symmetry with space group $I4_1/amd$ the same as that of bulk crystal. Note that the particle sizes of the Mn_3O_4 nanoparticles were estimated based on the peak positions and the full widths at half maximum of the Bragg peaks using Scherrer's equation. These results indicated successful synthesis the Mn_3O_4 nanoparticles with mean particle size of d = 7.8, 11.4, and 18.3 nm.

FIG. 1 HERE (Note white space above and below.)

The lattice constants a and c of the nanoparticles were estimated from XRD patterns. The observed broad diffraction peaks were deconvoluted to those associated with Mn_3O_4 by multi-peak fitting. The lattice constants were calculated from the relation between the lattice constants and the plane indices determined from the Bragg peak angles for all the deconvoluted peaks. The estimated lattice constants are listed in Table I. The lattice constants for the nanoparticles were slightly different from those for bulk crystal [4] and depended on the particle size. Compared with the lattice constants for bulk crystal, the deviation of value of c is larger than that of a, which indicated that the crystallographic structure for the nanoparticle is distorted from the bulk crystal. In particular, for d = 7.8 and 11.4 nm, the lattice constant a is larger than that for bulk crystal, while c is smaller than that for bulk crystal. The lattice constant a for d = 7.8 nm was slightly larger than that for d = 11.4 and 18.3 nm, while the c for d = 7.8 and 11.4 nm were similar value and slightly larger than that for d = 18.3 nm. The results indicate that the lattice distortion for the Mn_3O_4 nanoparticles increases as particle size decreases. The tetragonal distortion has been used to describe the Jahn-Teller distortion in Mn_3O_4. The Mn_3O_4 bulk crystal has huge tetragonal distortion, $c/(\sqrt{2}\ a)$ = 1.162 [4]. The estimated tetragonal distortion for the nanoparticles listed in Table I indicates that the Jahn-Teller distortion for Mn_3O_4 nanoparticles is suppressed as compared with the bulk crystal, and its magnitude decreases with decreasing particle size.

TABLE 1 HERE (Note white space above and below.)

The DC magnetic susceptibilities for the nanoparticles were measured under an external magnetic field H = 200 Oe in both field cooling (FC) and zero-field-cooling (ZFC) conditions. Fig. 2(a) shows the temperature dependence of the Mn_3O_4 nanoparticles with d = 11.4 nm. The susceptibility exhibited a clear hysteresis between FC and ZFC conditions. Both the FC and ZFC susceptibilities exhibited a rapid increased at around T = 42 K, corresponding to the T_N for bulk crystal, which is the onset of the Yafet-Kittel phase. In addition, the ZFC susceptibility exhibited the two anomalies at around 40 K as shown in inset of Fig. 2 (a), which correspond to the transition temperatures T_1 and T_2 as described later. Fig. 2(b) shows temperature dependence of FC susceptibilities for the three nanoparticles, which suggest that the T_N of 7.8 nm is lower than those of 11.4 and 18.3nm. The magnetic ordering temperatures were estimated by temperature differentiation of ZFC susceptibility as shown in Fig. 2(c) [6,12]. The $d\chi_{ZFC}/dT$ curves for d = 11.4 nm shows three peaks corresponding to the T_N = 42.4 K, T_1 = 40.9 K, and T_2 = 39.3 K, respectively. The evaluated magnetic transition temperatures are listed in Table II. Compared with the bulk crystal [6], the T_N and T_1 are almost the same as those of bulk crystal, while the T_2 is slightly higher than that of bulk crystal. For d = 18.3 nm, the $d\chi_{ZFC}/dT$ curves also shows three peaks, and those transition temperatures are almost same values as those for d = 11.4 nm. However, the $d\chi_{ZFC}/dT$ curves for d = 7.8 nm exhibit distinct two peaks at 40 K corresponding to the T_N and 34.5 K corresponding to the T_1 or T_2, which suggests the disappearance of the IC or CD phase for nanoparticles with d = 7.8 nm. In the case of Mn_3O_4 thin films [12], the dM/dT curves of thickness of 8 and 25 nm exhibit three peaks corresponding to the three transition temperatures, while that of thickness of 4 nm exhibits a peak only. The transition temperature for 4 nm was larger than that for 8 and 25 nm. The authors concluded that the behavior for thin film with thickness of 4 nm was associated with the surface roughness, which could greatly destroy the exchange interactions among the Mn ions. Hence, the T_N for the thinnest is lower than that of the thicker film [12]. In this study, it is considered that the decrease in the transition temperatures for the nanoparticles with d = 7.8 nm is attributed to the surface state.

FIG. 2 HERE (Note white space above and below.)

The magnetization curves for the nanoparticles were measured ranging from 5 to -5 T. Fig. 3 shows the magnetization curves for the nanoparticles at 5 K. The magnetization curves exhibited a hysteresis loop below T_N. The values of coercive filed H_c at 5 K are listed in Table II. The H_c for the d = 11.4 and 18.3 nm were almost same value, which was rather larger than that for 7.8 nm. The obtained H_c is quite larger than that for powdered bulk polycrystalline, H_c = 4980 Oe. This behavior is similar to previous studies for the nanoparticle [13,14] and thin film [12,15]. In the case of the previous investigations for Mn_3O_4 nanoparticles, it is

concluded that the increases in the coercive field are attributed to the significant increase in specific surface, such that the magnetic surface anisotropy is enhanced [13,14].

FIG. 3 HERE (Note white space above and below.)

The crystal structural analysis results indicated that the lattice constants and Jahn-Teller distortion depended on the particle size and exhibited the pronounced change at 7.8 nm, while those values were almost constant above 11.4 nm. The nanoparticles for d = 11.4 and 18.3 nm exhibited the three pronounced magnetic transition temperatures, while the nanoparticles for d = 7.8 nm exhibited two transition temperatures. In addition, the values of the transition temperatures and the coercive field for d = 7.8 nm was rather lower and smaller than those for d = 11.4 and 18.3 nm, respectively. These results indicated that the magnetic properties for the Mn_3O_4 nanoparticles exhibited pronounced changes below 7.8 nm. The experimental results suggest the Mn_3O_4 nanoparticles have strong correlation between crystal structure and magnetic property. As particle size decreases, the changes in the crystal structure and electronic state should be induced because of the enhancement of influence of surface state, which results in the remarkable changes in the lattice constants, Jahn-Teller distortion, and magnetic properties for the nanoparticles of d = 7.8 nm. The transition temperature T_2 for the nanoparticles is higher than that for bulk crystal. It is considered that the increases in the transition temperatures are attributed to the decreasing of atomic distances and enhancing the exchange interactions of Mn atoms owing to the reduction of the lattice constants [12]. On the other hand, the Mn_3O_4 has a tetragonal distortion combined with Jahn-Teller distortion. The Mn^{3+} spins at the MnO_6 octahedra having antiferromagnetic interactions with each other on the corner of a tetragonally distorted tetrahedron give rise to two possible energetically degenerate spin configurations, resulting in the increase in the spin fluctuation above T_N and its decrease with successive magnetic phase transitions [3]. In the case of the nanoparticles of $DyMnO_3$ with orthorhombic distortion of perovskite structure associated with the Jahn-Teller distortion, the size dependences of magnetic properties are related to the reduction of the lattice distortion [8]. Moreover, the Mn_3O_4 bulk crystal shows magnetic field induced crystal structural- and magnetostructural-modulation and magnetic phase transition [1,2]. The structural phase transition is associated with a rearrangement of frustrated one-dimensional antiferromagnetic chains composed by B-site Mn^{3+} [2]. In addition, the structural- and magnetic- phase transition is also induced under high pressure for bulk crystal and nanoparticle [1,5,16]. Compared with bulk crystal, the Mn_3O_4 nanoparticles with $d \sim 10$ nm show an elevation of phase transition pressure and different phase diagram, which are derived from unique atomic configuration and higher surface energy together with the nano-size effect [5]. In this study, the decrease in the Jahn-Teller distortion for d = 7.8 nm is presumed to induce the change in the orbital degeneracy of the e_g states in Mn^{3+} ions. Therefore, the modulation of the lattice constants and reduction of the Jahn-Teller distortion varies the magnetic interactions between the Mn spins, which result in the pronounced changes in the transition temperatures, coercive field and magnetic phase diagram. By continuing statistical research on Mn_3O_4 nanoparticles with other particle sizes, we are planning to understand the size effect of Mn_3O_4 nanoparticles in more detail.

TABLE 2 HERE (Note white space above and below.)

IV. CONCLUSION

We synthesized the Mn_3O_4 nanoparticles with d = 7.8, 11.4, and 18.3 nm in the pores of mesoporous silica SBA-15 and investigated their crystallographic structure and magnetic property. The XRD patterns of the three nanoparticles exhibited the tetragonal symmetry similarly to the bulk crystal at room temperature. The lattice constants for the nanoparticles were slightly different from those for bulk crystal and depended on particle size. The lattice constants change significantly at 7.8 nm, in addition, the tetragonal distortion associated with Jahn-Teller distortion decreases at 7.8 nm. The magnetic properties exhibited pronounced changes at 7.8 nm. The temperature dependences of DC magnetic susceptibility exhibited the successive phase transformations. The nanoparticles with d = 11.4 and 18.3 nm clearly exhibited the three transition temperatures, whereas the nanoparticles with d = 7.8 nm exhibited the two transition temperatures. The magnetization curve for the nanoparticles exhibited a hysteresis loop at below T_N. The coercive field for d = 11.4 and 18.3 nm was almost the same value, and its value for d = 7.8 nm decreased significantly. These experimental results suggested that the Mn_3O_4 nanoparticles with d = 7.8-18.3 nm have a strong correlation between the crystallographic structure and magnetic properties. The reduction of the tetragonal lattice distortion associated with Jahn-Teller distortion results in the changes in the magnetic transition temperature, coercive field, and magnetic phase diagram.

ACKNOWLEDGMENT

The synchrotron radiation experiments were performed at the beamline BL-8B in the Photon Factory (Proposal No. 2017G027).

REFERENCES

[1] M. Kim, X. M. Chen, X. Wang, C. S. Nelson, R. Budakian, P. Abbamonte, and S. L. Cooper, "Pressure and field tuning the magnetostructural phases of Mn_3O_4: Raman scattering and x-ray diffraction studies," *Phys. Rev.* B, vol. 84, pp. 174424, 2011.

[2] Y. Nii, H. Sagayama, H. Umetsu, N. Abe, K. Taniguchi, and T. Arima, "Interplay among spin, orbital, and lattice degrees of freedom in a frustrated spinel Mn_3O_4," *Phys. Rev. B*, vol. 87, pp. 195115, 2013.

[3] Y. Ishitsuka, T. Ishikawa, R. Koborinai, T. Omura, and T. Katsufuji, "Comparative studies of the thermal conductivity of spinel oxides with orbital degrees of freedom," *Phys. Rev. B*, vol. 90, pp. 224411, 2014.
[4] M. C. Kemei, J. K. Harada, R. Seshadri, and M. R. Suchomel, "Structural change and phase coexistence upon magnetic ordering in the magnetodielectric spinel Mn_3O4," *Phys. Rev. B*, vol. 90, pp. 064418, 2014.
[5] H. Lv, M. Yao, Q. Li, Z. Li, B. Liu, R. Liu, S. Lu, *et al.*, "Effect of Grain Size on Pressure-Induced Structural Transition in Mn_3O_4," *J. Phys. Chem. C*, vol. 116, pp. 2165-2171, 2011.
[6] J.-H. Chung, K. H. Lee, Y.-S. Song, T. Suzuki, and T. Katsufuji, "Low Temperature Structural Instability of Tetragonal Spinel Mn_3O_4," *J. Phys. Soc. Jpn*, vol. **82**, pp. 034707, 2013.
[7] T. Tajiri, H. Deguchi, S. Kohiki1, M. Mito, S. Takagi, K. Tsuda, and Y. Murakami, "Novel Size Effect of $LaMnO_{3+\delta}$ Nanocrystals Embeded in SBA-15 Mesoporous Silica," *J. Phys. Soc. Jpn*, vol. **75**, pp. 113704, 2006.
[8] T. Tajiri, N. Terashita, K. Hamamoto, H. Deguchi, M. Mito, Y. Morimoto, et al., "Size dependences of crystal structure and magnetic properties of $DyMnO_3$ nanoparticles," *J. Magn. Mnagn. Mater.*, vol. **345**, pp. 288, 2013.
[9] T. Tajiri, S. Saisho, M. Mito, H. Deguchi, K. Konishi, and A. Kohno, "Size Dependence of Crystal Structure and Magnetic Properties of NiO Nanoparticles in Mesoporous Silica," *J. Phys. Chem. C*, vol. **119**, pp. 1194, 2015.
[10] T. Tajiri, Y. Ando, H. Deguchi, M. Mito, and A. Kohno, "Magnetic Properties and Crystal Structure of $DyMn_2O_5$ Nanoparticles Embedded in Mesoporous Silica"
[11] D. Zhao, J. Feng, Q. Huo, N. Melosh, G. H. Fredrickson, B. F. Chemlka, and G. D. Stucky, "Triblock Copolymer Syntheses of Mesoporous Silica with Periodic 50 to 300 Angstrom Pores," *science*, vol. **279**, pp. 548 1998.
[12] L. Ren, M. Yang, W. Zhou, S. Wu, and S. Li, "Influence of Stress and Defect on Magnetic Properties of Mn_3O_4 Films Grown on $MgAl_2O_4$ (001) by Molecular Beam Epitaxy," *J. Phys. Chem. C*, vol. **118**, pp. 243, 2013.
[13] B. Chen, G. Rao, S. Wang, Y. Lan, L. Pan, and X. Zhang, "Facile synthesis and characterization of Mn_3O_4 nanoparticles by auto-combustion method," *Mater. Lett.*, vol. **154**, pp. 160, 2015.
[14] R. Song, S. Feng, H. Wang, C. Hou, "Effect oforganicsolventsonparticlesize of Mn_3O_4 nanoparticles synthesized by a solvothermal method," J. Solid State Chem., vol. **202**, pp.57, 2013.
[15] L.W. Guo, D.L. Peng, H. Makino, K. Inaba, H.J. Ko, K. Sumiyama, and T. Yao, "Structural and magnetic properties of Mn_3O_4 films grown on MgO(0 0 1) substrates by plasma-assisted MBE," J. Magn. Magn. Mater., vol. **213**, pp. 321, 2000.
[16] J. Darul, C. Lathe, and P. Piszora, "Mn_3O_4 under High Pressure and Temperature: Thermal Stability, Polymorphism, and Elastic Properties," J. Phys. Chem. C **117**, 23487 (2013).

TABLE I
LATTICE CONSTANTS AND TETRAGONAL DISTORTION

d [nm]	*a* [Å]	*c* [Å]	$c/\sqrt{2}\,a$
7.8	5.780(1)	9.448(5)	1.156
11.4	5.765(1)	9.445(1)	1.159
18.3	5.762(1)	9.432(1)	1.158
bulk [4]	5.76289(1)	9.46885(1)	1.162

Lattice constants, *a* and *c*, of tetragonal symmetry and tetragonal distortion, $c/\sqrt{2}\,a$, for the nanoparticle and bulk crystal at room temperature. The values for bulk crystal are referred from Ref. 4.

TABLE II
MAGNETIC TRANSITION TEMPERATURES AND COERCIVE FIELD

d [nm]	T_N [K]	T_1 [K]	T_2 [K]	H_c [Oe]
7.8	40.0	34.5		8190
11.4	42.4	40.9	39.3	8740
18.3	42.6	41.7	39.7	8790
bulk	43.9 [6]	41.2 [6]	35.0 [6]	4980

Magnetic transition temperatures and coercive field at 5 K for the nanoparticles and bulk crystal. The transition temperatures is estimated by temperature differentiation of ZFC susceptibility. For *d* = 7.8 nm, the lower transition temperature is corresponding to the T_1 or T_2. The transition temperatures for the bulk crystal are referred from Ref. 6.

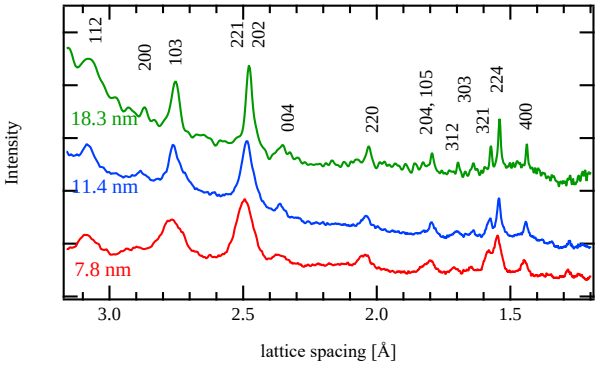

Fig. 1. XRD patterns for the Mn_3O_4 nanoparticles with *d* = 7.8, 11.4, and 18.3 nm at room temperature.

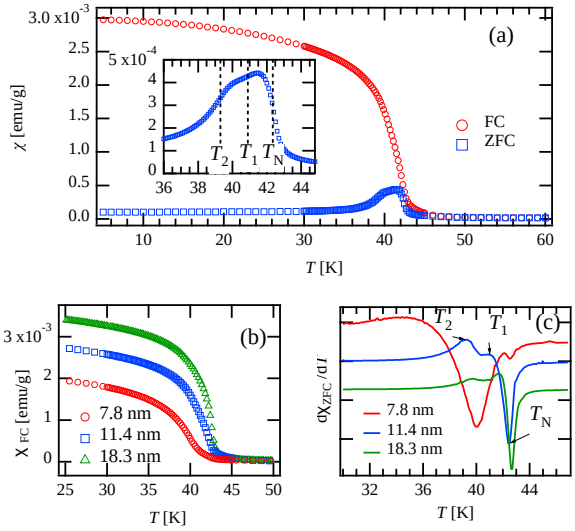

Fig. 2. (a) Temperature dependence of DC susceptibility for the nanoparticles with *d* = 11.4 nm under magnetic field *H* = 200 Oe in FC and ZFC conditions. Inset shows a magnification of ZFC susceptibility near the transition temperatures. (b) Temperature dependence of susceptibility for *d* = 7.8, 114, and 18.3 nm under FC condition. (c) Temperature dependence of derivative curve $d\chi_{ZFC}/dT$.

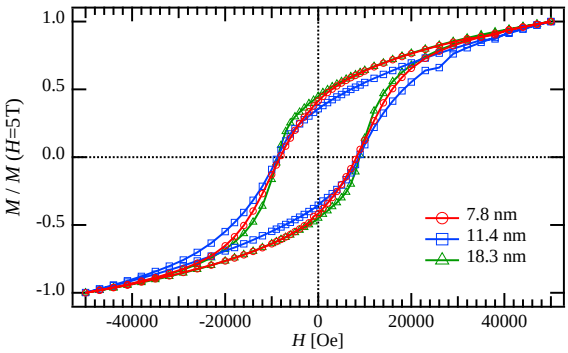

Fig. 3. Magnetization curves for the Mn_3O_4 nanoparticles at 5 K.